

Article

Effect of Flow Rate and Partial Pressure of Oxygen on Desulfurization of KR Slag

Peng Jiang¹, Jiajun Jiang², Rodrigue Armel Muvunyi² and Jianli Li^{2,3,*} ¹ Jiangsu Yonggang Group Co., Ltd., Zhangjiagang 215628, China; jtw@wust.edu.cn² Hubei Provincial Key Laboratory for New Processes of Ironmaking and Steelmaking, Wuhan University of Science and Technology, Wuhan 430081, China; jiajun@wust.edu.cn (J.J.); rodriguearmel5@wust.edu.cn (R.A.M.)³ Key Laboratory for Ferrous Metallurgy and Resources Utilization of Ministry of Education, Wuhan University of Science and Technology, Wuhan 430081, China

* Correspondence: jli@wust.edu.cn

Abstract: KR (Kanbara Reaction) desulfurization slag is a solid waste that is not sufficiently utilized. This is because the KR desulfurization slag contains 1–2.5% sulfur, which is directly used in steel smelting to increase the sulfur content in molten steel. Therefore, the possibility of oxidation desulfurization of KR desulfurization slag was studied in this study. Experiments were conducted to investigate the possibility of removing sulfur from used KR (Kanbara Reaction) slag with oxidation. The KR slag samples were treated with oxidative desulfurization in the oxygen partial pressure range of 0.05 bar–1.00 bar, with a gas flow rate ranging from 2 L min⁻¹ to 6 L min⁻¹, and at a temperature of 1420 °C. X-ray diffraction (XRD), an infrared carbon sulfur analyzer, and scanning electron microscopy–energy dispersive X-ray spectrometry (SEM–EDS) analysis were used to reveal the oxidative desulfurization mechanism of KR desulfurization slag. At low oxygen pressure ($P_{O_2} < 0.20$ bar), the desulfurization rate of slag oxidized for 120 min increased with the increase in oxygen partial pressure. At high oxygen pressure ($P_{O_2} \geq 0.20$ bar), the desulfurization rate of slag samples did not change with the change in oxygen partial pressure, and the desulfurization rate was higher than 93.5%. At low oxygen pressure ($P_{O_2} < 0.20$ bar), the residual sulfur in the slag after oxidation still existed in the slag as the CaS phase. At high oxygen pressure ($P_{O_2} \geq 0.20$ bar), the residual sulfur in the slag oxidized from the CaS phase to the 11CaO·7Al₂O₃·CaS phase in the slag. The sulfur removal rate was directly correlated with the slag surface area and the flow rate of the reaction gas, and it increased with an increase in both surface area and gas flow rate.

Keywords: KR slag; oxygen pressure; oxidation behavior; desulfurization

Citation: Jiang, P.; Jiang, J.; Muvunyi, R.A.; Li, J. Effect of Flow Rate and Partial Pressure of Oxygen on Desulfurization of KR Slag. *Metals* **2024**, *14*, 516. <https://doi.org/10.3390/met14050516>

Academic Editors: Farshid Pahlevani and Smitirupa Biswal

Received: 16 March 2024

Revised: 23 April 2024

Accepted: 25 April 2024

Published: 28 April 2024



Copyright: © 2024 by the authors. Licensee MDPI, Basel, Switzerland. This article is an open access article distributed under the terms and conditions of the Creative Commons Attribution (CC BY) license (<https://creativecommons.org/licenses/by/4.0/>).

1. Introduction

In recent years, environmental protection and sustainable development have been highly valued worldwide. It is important to properly handle industrial by-products and effectively convert them into green materials. A large amount of solid waste, such as pulverized blast furnace slag, desulfurized slag, and steel slag, is produced in the process of desulfurization and converter steelmaking. The Kanbara Reactor (KR) desulfurization process is widely used in various steel plants as an efficient pre-desulfurization process before the converter process [1–7]. In the KR desulfurization process, an impeller lined with refractory material is submerged in the ladle, where it rotates and stirs the hot metal to create a vortex. The solid waste produced by the KR desulfurization process is called KR desulfurization slag. In Taiwan alone, the annual production of KR desulfurization slag amounts to approximately 340,000 tons [8]. For every ton of hot metal processed, the desulfurization pretreatment generates about 7–9 kg of KR desulfurization slag in steel production [9]. Figure 1 shows the production process of KR desulfurization slag.

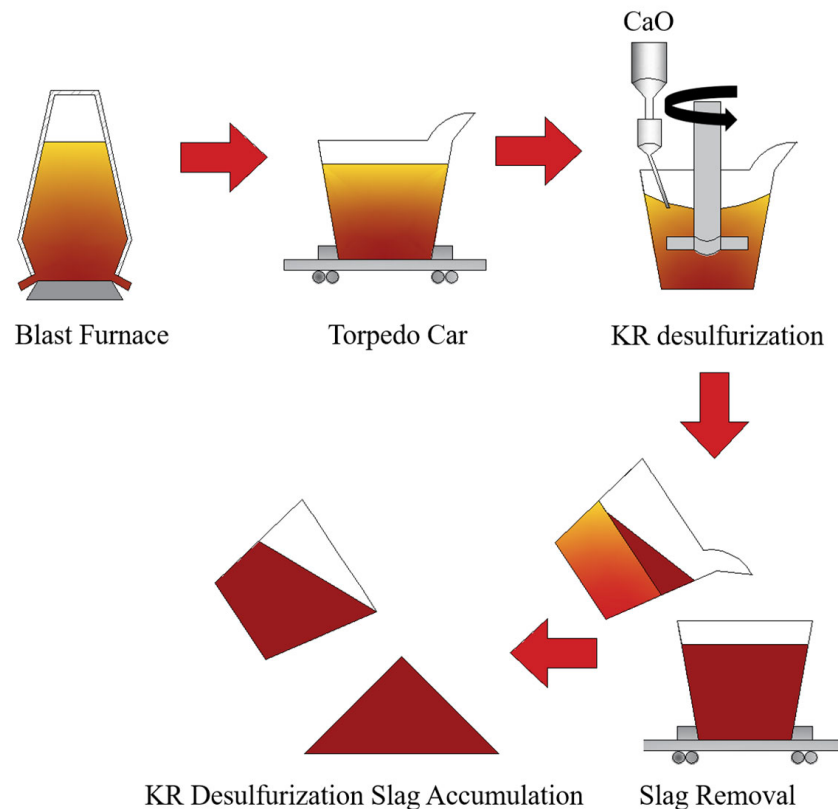


Figure 1. The production process of KR desulfurization slag.

KR desulfurization slag is a corrosive industrial residue (pH = 12.5) [10], which is considered a hazardous waste when its pH is higher than 12.5. Therefore, many scholars have studied the different methods of utilizing KR desulfurization slag. Fujino et al. [11] used KR desulfurization slag for the preparation of sintering raw materials. In addition, Nakai et al. [12] proposed a process in which hot KR desulfurization slag is directly reused for hot metal pretreatment. Kuo et al. [13] used KR desulfurization slag for soil improvement. In addition, Shiha et al. [8] also used KR desulfurization slag to replace the natural fine aggregates in ready-mixed soil components. In addition, KR desulfurization slag was used for soil backfill and cement clinker production. However, the overall utilization rate of KR desulfurization slag for these applications is low. Therefore, developing and improving a new process of KR desulfurization slag utilization will help solve the problems of the large accumulation of KR desulfurization slag and serious pollution in enterprises.

Research on the removal of sulfur from desulfurization slag is relatively new, but the interaction between gaseous components and sulfur in various liquid slags has been explored extensively. The release of sulfur from liquid blast furnace slags into the gas phase has also been extensively examined. For instance, Pelton et al. [14] investigated the kinetics of SO_2 evolution from synthetic slags in an O_2 and Ar atmosphere, noting a rapid desulfurization rate at low oxygen partial pressures, which slowed significantly at higher pressures. Further, Agrawal et al. [15] explored the desulfurization of these slags using Ar– H_2O mixtures at 1400 °C.

In the context of oxidation reactions, studies have shown that sulfur primarily exists as CaS in desulfurization slags. Lynch et al.'s [16] work on CaS oxidation in an O_2 and Ar atmosphere across temperatures from 1050 °C to 1580 °C demonstrated that, at high temperatures and low oxygen partial pressures, CaS converts to CaO and SO_2 , while at lower temperatures and higher oxygen partial pressures, it forms CaSO_4 .

The focus of this work is to investigate the oxidation of sulfur in KR desulfurization slag using O_2 at 1420 °C in the range of oxygen partial pressures of 0.10 bar–1.00 bar and in the range of flow rates of 2 L min^{-1} –6 L min^{-1} . The purpose is to recover slag from

iron and steel metallurgy by removing sulfur from slag and to provide new insights into scalable applications.

2. Experimental Section

2.1. Materials

Table 1 shows the composition of the synthetic slag sample prepared by the experiment. The reagent used in the present study was supplied by Sinopharm Group. CaO, SiO₂, MgO, Al₂O₃, and CaF₂ (Sinopharm Chemical Reagent Co., Ltd. Wuhan China) were analytically pure chemical reagents, except for the CaS in the slag, which was prepared by the laboratory. Figure 2 shows a schematic diagram of the experimental procedure for the laboratory preparation of CaS. It used CaSO₄ (purity > 99.95%) and carbon powder (purity > 99.85%), which was n (CaSO₄): n (Carbon Powder) = 2:1 (n—the amount of substance). The reaction temperature of the experiment was 1100 °C for 120 min, and the furnace was under an atmosphere of high purity N₂ for which the flow rate was 10 L min⁻¹. The gases used in this study were pure oxygen and nitrogen (with purity levels of 99.999% and 99.999%, respectively, supplied by the flying cloud process).

Table 1. Composition of synthetic slag/wt%. Reprinted from ref. [17].

Basicity	CaO	SiO ₂	Al ₂ O ₃	MgO	CaS	CaF ₂
3.5	62.73	17.92	6.00	3.00	3.38	6.97

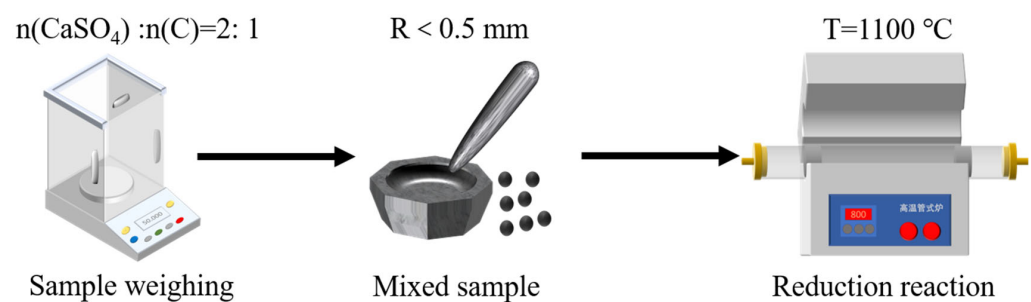


Figure 2. Schematic of CaS process for laboratory preparation.

The analytically pure chemical reagents were calcinated at 1000 °C for at least 2 h before the sample preparation. The chemically pure reagents and the laboratory-prepared CaS were accurately weighed, which was followed by a meticulous homogenous mixing of the components in a corundum crucible. Subsequently, the crucible, housing the prepared sample, was positioned within the temperature-controlled zone of a high-temperature carbon tube furnace. A nitrogen barsosphere was employed in the carbon tube furnace, with a nitrogen flow rate set at 5 L min⁻¹. The samples underwent controlled heating in the furnace, with a programmed heating rate of 15 °C min⁻¹. The temperature was gradually increased to 1600 °C and maintained for 15 min. The slag sample was extracted by a quartz glass tube when the holding time reached 15 min. The resulting slag samples were then collected for oxidation experiments.

2.2. Experimental Equipment

Figure 3 shows the structure of the high-temperature quenching furnace equipment in the laboratory. Only the salient features of the setup are described, while the details can be found in previous publications [17]. The equipment is composed of a gas supply system, control panel, and furnace body.

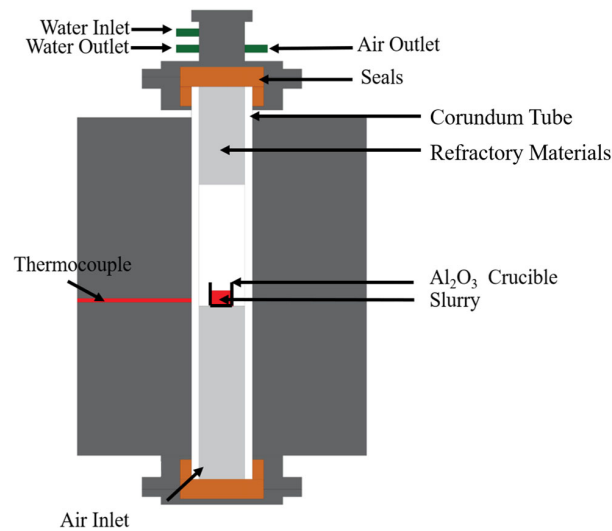


Figure 3. Equipment structure of the quenching furnace. Adapted from ref. [17].

2.3. Oxidation Experiments

The slag sample was put into either an Al_2O_3 crucible boat or an Al_2O_3 crucible. In the experiment, the liquid phase was the main phase ($1420\text{ }^\circ\text{C}$), but fixed-size slag was still used. The oxidation experimental process is shown in Figure 4. Before the experiment started, a high-purity nitrogen protection gas was injected into the furnace at a flow rate of 0.5 L min^{-1} , and the furnace was purged for 12 h. The furnace commenced heating, with a gradual temperature increase at a rate of $5\text{ }^\circ\text{C min}^{-1}$. After 10 min of heating, the adjustment of the oxygen partial pressure within the furnace was carried out. A total of 15 g of the slag sample was precisely measured and placed into either an Al_2O_3 crucible or an Al_2O_3 crucible boat. Figure 5 shows a schematic diagram of the crucible shape. Once the furnace temperature reached the designated set point, the crucible was introduced into the stable temperature zone within the furnace. Subsequently, the samples were positioned within the constant temperature zone. To assess the impact of the holding time on the experiment, varied oxidation durations were employed for low oxygen pressure (0.05 bar) and high oxygen pressure (0.5 bar) conditions (30 min, 60 min, 90 min, 120 min). The reaction gas comprised either pure O_2 or an $\text{O}_2\text{-N}_2$ mixture, and the overall gas flow rate ranged from 2 to 6 L min^{-1} . After the sample was allowed to oxidize for a predetermined amount of time, it was quickly moved outside the furnace. After processing, the oxidized sample was delivered to the appropriate instrument for examination.

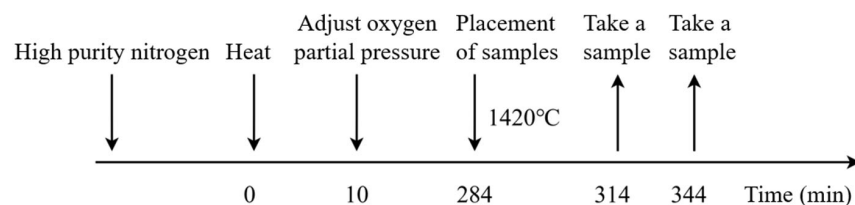


Figure 4. Schematic of oxidation experiment procedure.

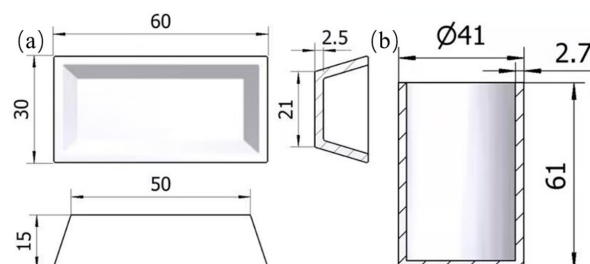


Figure 5. Schematic diagram of crucible shape: (a) crucible boat, (b) crucible.

3. Experiment Results

3.1. Removal Rate of Sulfur from Slag

The experiments were conducted at a temperature of 1420 °C. Pure oxygen (O₂) and oxygen–nitrogen (O₂–N₂) mixtures were utilized. Various flow rates of the reaction gas ranging from 2 to 6 L min^{−1} were employed. The initial sulfur content of the slag was 1.5% by mass. The experimental conditions are summarized in Table 2.

Table 2. Summary of experimental conditions and sulfur removal.

Sample	Crucible Shape	O ₂ (bar)	Reaction Time (min)	Gas Flow (L min ^{−1})	R _S (%)
S-1	Boat	0.5	30	2	47.58
S-2	Boat	0.5	60	2	70.23
S-3	Boat	0.5	90	2	85.84
S-4	Boat	0.5	120	2	93.06
S-5	Boat	0.05	30	2	8.79
S-6	Boat	0.05	60	2	20.90
S-7	Boat	0.05	90	2	45.88
S-8	Boat	0.05	120	2	66.88
S-9	Boat	0.1	120	2	75.95
S-10	Boat	0.15	120	2	79.11
S-11	Boat	0.20	120	2	93.62
S-12	Boat	0.25	120	2	97.51
S-13	Boat	0.5	120	2	93.56
S-14	Boat	0.75	120	2	96.51
S-15	Boat	1	120	2	95.47
S-16	Cylinder	0.5	30	2	39.59
S-17	Cylinder	0.5	60	2	67.14
S-18	Cylinder	0.5	90	2	80.40
S-19	Cylinder	0.5	120	2	85.97
S-20	Cylinder	0.5	30	4	63.69
S-21	Cylinder	0.5	60	4	74.10
S-22	Cylinder	0.5	90	4	84.05
S-23	Cylinder	0.5	120	4	89.09
S-24	Cylinder	0.5	30	6	64.05
S-25	Cylinder	0.5	40	6	66.19
S-26	Cylinder	0.5	50	6	69.975
S-27	Cylinder	0.5	60	6	74.48
S-28	Cylinder	0.5	90	6	83.58
S-29	Cylinder	0.5	120	6	90.56

3.2. Occurrence State of Residual Sulfur after Oxidation of Slag

Figure 6 shows the XRD patterns of the samples before and after oxidation. As shown in Figure 6, the main phases in the pre-oxidized slag samples are silicate phases (3CaO·SiO₂ and 2CaO·SiO₂), and S exists in the form of CaS. The main phases in the post-oxidized slag samples are 2CaO·SiO₂ phase and 11CaO·7Al₂O₃·CaF₂ phase.

Figure 7a shows the SEM photographs of the unoxidized samples. Figure 7b–f show the SEM photographs of 0.05 bar, 0.10 bar, 0.15 bar, 0.20 bar, and 0.75 bar after oxidation for 120 min. According to the EDS analysis, the predominant phases in the slag samples before oxidation included 3CaO·SiO₂ (phase 1), MgO (phase 2), the matrix phase (phase 3), and CaS (phase 4). After oxidation for 120 min under various oxygen partial pressures, the main phases observed in the slag samples were the matrix phase (phase 3), CaS (phase 4), and 2CaO·SiO₂ (phase 5). To explore the sulfur distribution within the samples, surface scanning analysis using SEM–EDS was conducted on the oxidized slag samples to elucidate the sulfur distribution within the slag, as illustrated in Figure 8.

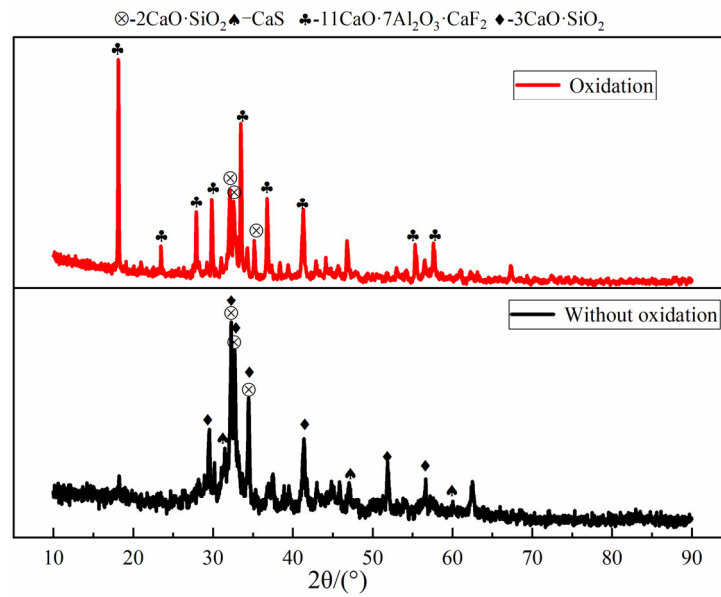


Figure 6. XRD patterns of the samples before and after oxidation.

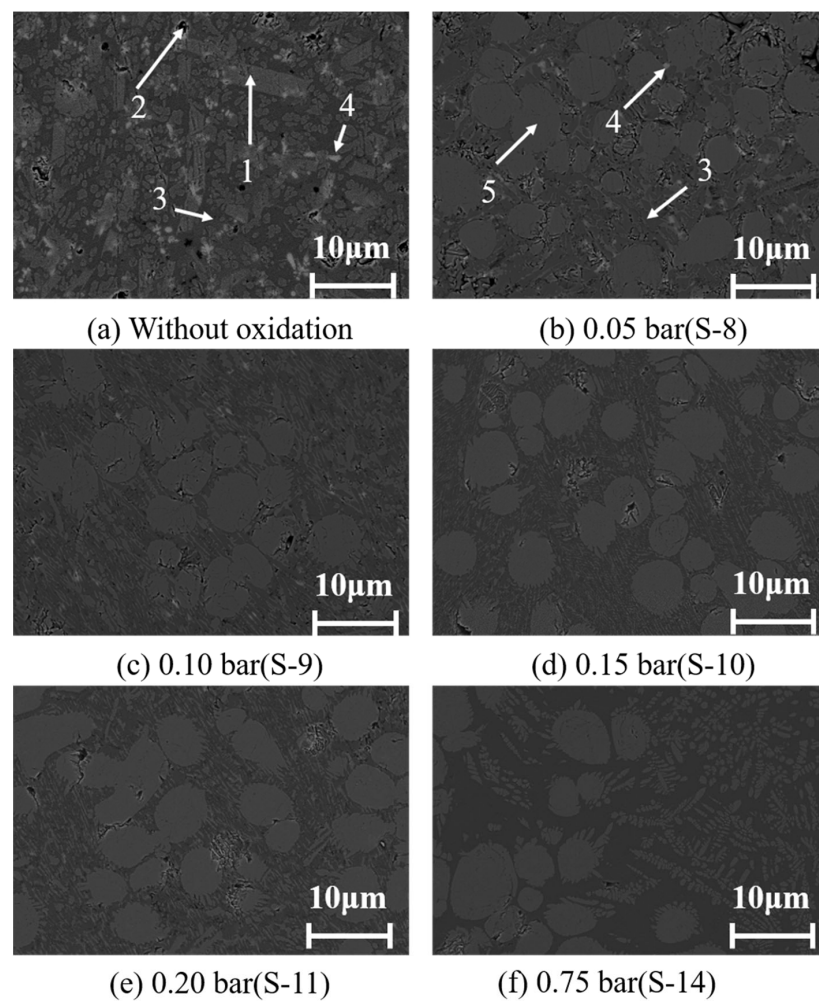


Figure 7. SEM microphotographs of slag (a) without oxidation, (b) oxidation at 0.05 bar, (c) oxidation at 0.10 bar, (d) oxidation at 0.15 bar, (e) oxidation at 0.20 bar, (f) oxidation at 0.75 bar (1: $3\text{CaO}\cdot\text{SiO}_2$ phase, 2: MgO phase, 3: Matrix phase, 4: CaS phase, 5: $3\text{CaO}\cdot\text{SiO}_2$ phase).

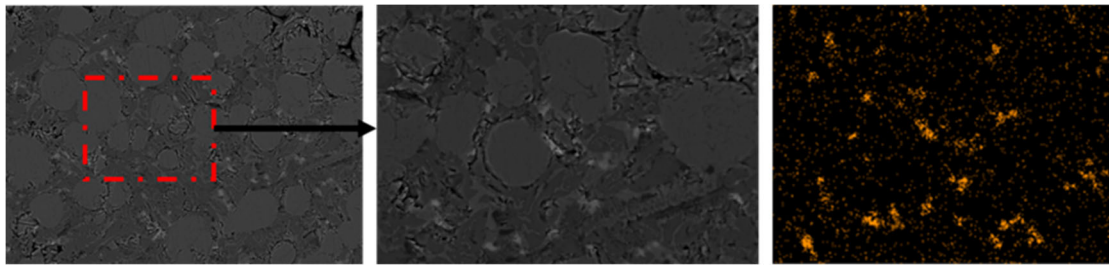


Figure 8. Surface scanning analysis of the sulfur elements in slag S-8 (0.05 bar oxidized for 120 min).

Analysis of Figure 8 indicates that elemental sulfur in the slag sample following oxidation under low oxygen pressure (0.05 bar) persists in the form of CaS. Under high oxygen pressure (0.5 bar), it was observed that elemental sulfur became concentrated in the newly formed physical phase 6 ($11\text{CaO}\cdot 7\text{Al}_2\text{O}_3\cdot \text{CaS}$) during the oxidation process. The surface scan of physical phase 6 is depicted in Figure 9.

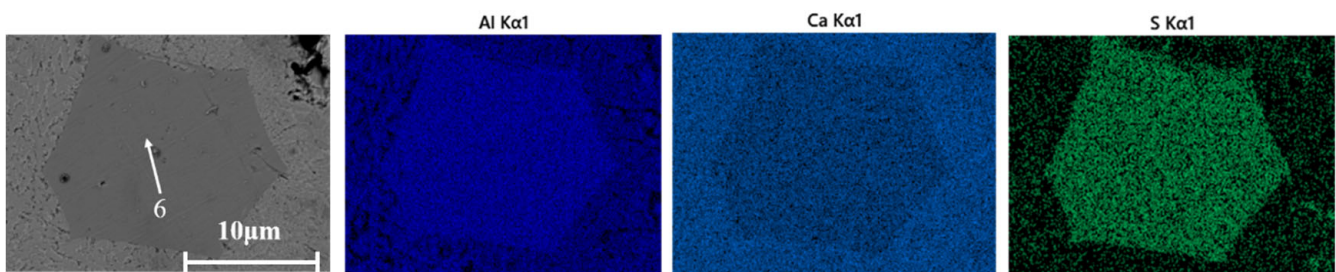


Figure 9. Surface scanning analysis of sulfur-containing occurrence phase elements in S-17 slag (0.5 bar oxidized for 60 min, 6: $11\text{CaO}\cdot 7\text{Al}_2\text{O}_3\cdot \text{CaS}$ phase).

Throughout this study, the sulfur removal degree, denoted as R_S and defined in Equation (1), is employed to quantify sulfur removal:

$$R_S = \frac{(S_i - S_f)}{S_i} \times 100\% \quad (1)$$

where S_i is the sulfur content of the original slag and S_f is the sulfur content in the slag after the reaction.

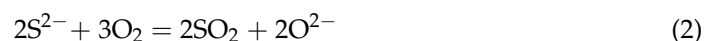
Table 2 also includes the experimentally achieved R_S values.

4. Discussion

4.1. Thermodynamic Analysis

The impact of the molar ratio of calcium sulfide to carbon dioxide at different temperatures was computed utilizing the Phase Diagram module within the thermodynamic database FactSage 8.1. The outcomes are presented in Figure 10. It can be seen that temperature and the number of O_2 moles are the main factors affecting the reaction products. According to previous research [11], sulfur in the slag can be effectively removed at 1420°C . As depicted in Figure 10, the CaS stable region (red circular region) decreases with an increase in the number of O_2 moles in the reaction system at a temperature of 1420°C . In summary, sulfur from KR desulfurization slag can be effectively oxidized to SO_2 and CaO by adjusting the partial pressure of oxygen in the reaction system.

Under the experimental conditions, the observed phenomenon indicates that the slag is in a liquid state. In such cases, sulfur in the slag is removed through oxidation, as depicted in Equation (2).



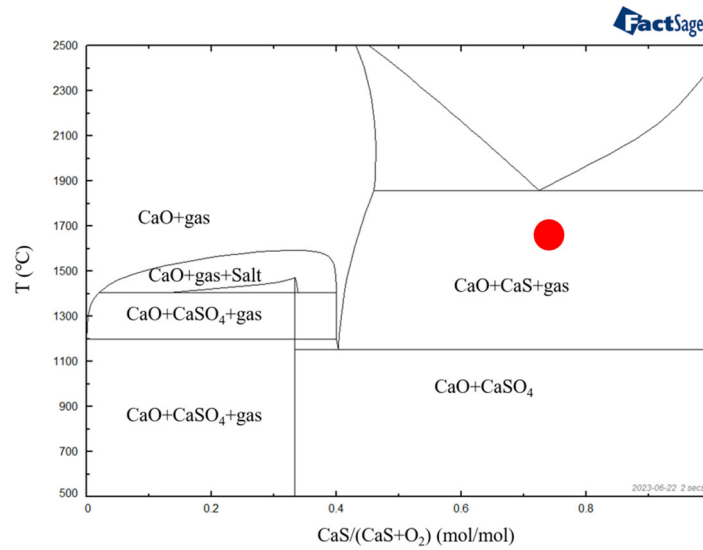


Figure 10. Phase composition of products with molar ratio of CaS to (CaS + O₂) at different temperatures.

Figure 11 is the calculation of the Ca–O–S stability diagram at 1420 °C using the predom module of the thermodynamic database FactSage 8.1. In the experimental setup, the barsphere within the reaction system is situated within the designated region (triangular region) on the dominance region diagram of Ca–O–S. The reaction products can be affected by changing the partial pressure of oxygen while keeping the temperature constant. To oxidatively remove sulfur from the slag, the reaction products must be CaO and SO₂ (CaSO₄ will remain in the slag). It can also be seen from Equation (2) that oxygen partial pressure has a significant effect on oxidative desulfurization. For Equation (2), the equilibrium constant is expressed as:

$$K_{(2)} = \frac{a_{O^{2-}}^2 \times P_{SO_2}^2}{a_{S^{2-}}^2 \times P_{O_2}^3} \quad (3)$$

where $K_{(2)}$ is the equilibrium constant of Equation (2), $a_{O^{2-}}$ is the activity of O²⁻ in the slag solution, $a_{S^{2-}}$ is the activity of S²⁻ in the slag solution, P_{SO_2} is the partial pressure of SO₂ in the reaction, and P_{O_2} is the partial pressure of O₂ in the reaction.

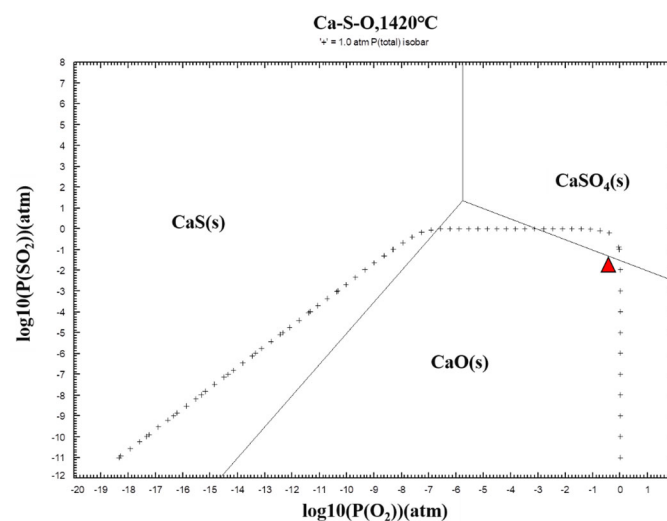


Figure 11. Stability diagram of the Ca–S–O system at 1420 °C.

The formula above shows how either lowering the partial pressure of SO₂ or raising the partial pressure of oxygen may lower the sulfur content in slag at a constant temperature. Under the existing experimental conditions, the partial pressure of SO₂ in the system can

be reduced by increasing the SO_2 gas exclusion rate. This rate is determined by three factors: (1) the gas flow rate, (2) the container's surface area, and (3) the separation between the liquid's surface and the crucible's edge. The forthcoming section will delve into the predominant factors influencing the desulfurization rate and the ultimate extent of sulfur removal from slag.

4.2. Removal Rate of Sulfur from Slag

From the preceding analysis, it is evident that the kinetic process of the desulfurization reaction under experimental conditions can be examined using a two-mode theory. In the research by Wei S K [18], CaS oxidative desulfurization is characterized as a first-order reaction, and the kinetic diagram of the desulfurization reaction is depicted in Figure 12. Figure 12 depicts the stages of the reaction process as follows: (1) O_2 diffuses from the gas phase to the gas–liquid interface, (2) O_2 further diffuses from the gas–liquid interface into the liquid phase where the reaction takes place, (3) S^{2-} migrates from the bulk liquid phase to liquid film and undergoes a reaction with dissolved O_2 during the diffusion process, and (4) SO_2 diffuses toward the interface and enters the gas phase.

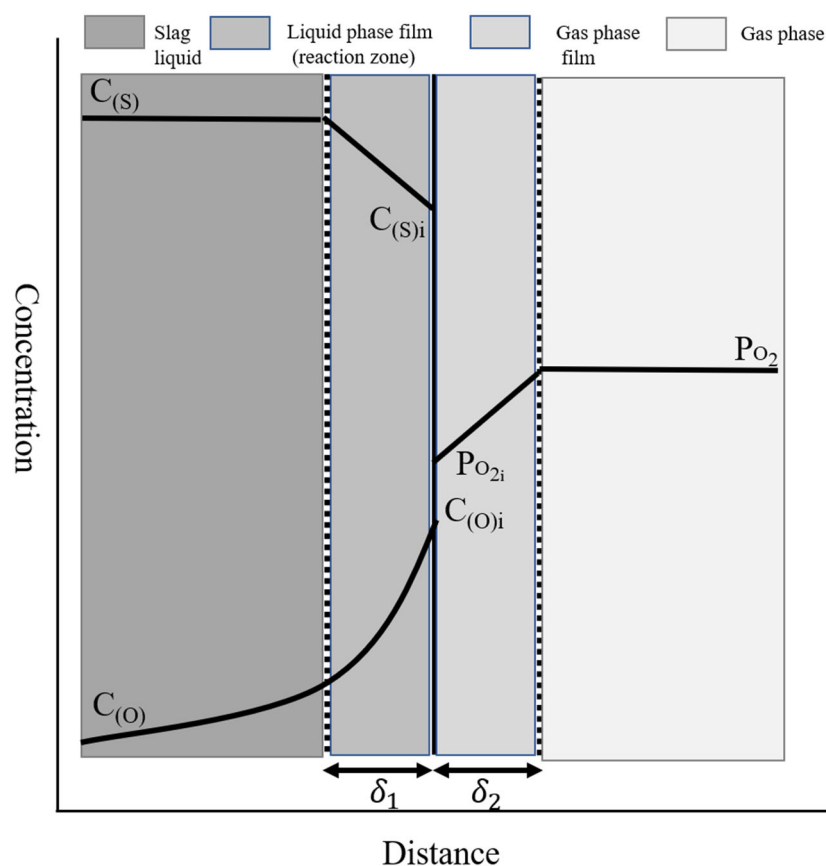


Figure 12. Schematic diagram illustrating the dynamics of slag oxidative desulfurization reaction.

Given that the reaction occurs at high temperatures and under conditions of heterogeneous nucleation, the interfacial reaction and SO_2 escaping into the gas phase via the liquid–gas interface process are not the rate-limiting steps. Instead, the reaction rate is predominantly governed by the mass transfer rate across the gas–liquid phase boundary layer. With the mass transfer theory, the mass transfer rate of oxygen in the gas phase and the sulfur mass transfer process in the slag phase can be represented by Equation (4) and Equation (5), respectively. Since the interface reaction rate is very fast, it can be considered

that $P_{O_{2i}} \approx 0$ and $C_{S_i} \approx 0$; under this condition, Equations (4) and (5) are simplified to (6) and (7), respectively.

$$J_{O_2} = \frac{k_{O_2}}{RT} (P_{O_2} - P_{O_{2i}}) \quad (4)$$

$$J_S = k_S (C_S - C_{S_i}) \quad (5)$$

$$J_{O_2} = \frac{k_{O_2}}{RT} P_{O_2} \quad (6)$$

$$J_S = k_S C_S \quad (7)$$

The ratio of the mass transfer rate of O_2 to that of S can be denoted as β , as expressed in Equation (8) as follows:

$$\beta = \frac{J_{O_2}}{J_S} = \frac{1}{C_S} \left(\frac{k_{O_2}}{k_S} \right) \left(\frac{P_{O_2}}{RT} \right) \quad (8)$$

where J_{O_2} is the mass transfer rate of O_2 , mol s^{-1} ; k_{O_2} is the mass transfer coefficient of O_2 , cm s^{-1} ; R is the gas constant, $\text{J (mol}\cdot\text{K)}^{-1}$; T is temperature, $^{\circ}\text{C}$; P_{O_2} is the partial pressure of oxygen in the gas phase, bar; $P_{O_{2i}}$ is the partial pressure of oxygen at the phase interface, bar; J_S is the mass transfer rate of S, mol s^{-1} ; k_S is the mass transfer coefficient of S, cm s^{-1} ; C_S is the concentration of S in the slag, mol cm^{-3} ; C_{S_i} is the concentration of S at the interface, mol cm^{-3} ; and β is the ratio of the mass transfer.

When $\beta < 1$, the mass transfer rate of O_2 is lower than that of S, leading to the reaction rate being predominantly influenced by the mass transfer rate of O_2 . Conversely, when $\beta > 1$, the mass transfer rate of O_2 surpasses that of S, thus making the reaction rate chiefly dependent on the mass transfer rate of S. Pelton et al. [14] investigated the kinetics of the sulfur oxidation process and established that under conditions of adequate oxygen supply, the governing factor in the sulfur oxidation process within slag was the diffusion control of S^{2-} in the liquid phase.

Figure 13 depicts the relationship between the desulfurization rate and the oxygen partial pressure of slag oxidized for 120 min, based on the data provided in Table 2. As can be seen from Figure 13, within the reaction system featuring an oxygen partial pressure ranging from 0.05 bar to 0.20 bar, the oxidation desulfurization rate of slag steadily increases with the elevation of oxygen partial pressure. Once the oxygen partial pressure of the reaction system reaches or exceeds 0.20 bar, the desulfurization rate of sulfur oxidation in the slag stabilizes above 93.5%. Moreover, as the oxygen partial pressure increases, the desulfurization rate of slag oxidation tends to stabilize, suggesting near-complete sulfur removal from the slag during the oxidation process under conditions of high oxygen partial pressure. Figure 14 shows the change in desulfurization degree with oxidation time at low oxygen partial pressure (0.05 bar) and high oxygen pressure (0.5 bar) after the oxidation of slag at 1420°C and a gas flow rate of 2 L min^{-1} . It can be seen that the growth rate of sulfur removal decreases with time. This decrease in the growth rate of the sulfur removal rate may be attributed to one factor: the slowdown in the mass transfer of sulfur from the bulk to the liquid surface as sulfur concentration decreases. With the decrease in sulfur concentration in the slag, the mass transfer rate of sulfur from the bulk to the liquid surface slows down. At the same time, when the oxygen partial pressure is 0.05 bar, the removal rate of sulfur in the slag is lower than for 0.5 bar oxygen partial pressure. Thus, the growth rate of sulfur removal decreases at 0.05 bar oxygen partial pressure. These findings deviate significantly from the recent reports by Allertz et al. [19] and Hiraki et al. [20]. Hiraki et al. reported a sulfur removal rate exceeding 90% after 60 min of reaction with an Ar- O_2 gas mixture (P_{O_2} was 0.21 bar) at 1100°C . Allertz et al. reported that sulfur oxidation removal from ladle slag was almost unaffected by oxygen partial pressure at 1400°C . Allertz also reported the effect of gas flow and the surface area of the container on the oxidation of sulfur in the slag. Nevertheless, there exist notable disparities in experimental conditions between the investigations conducted by Hiraki et al. and Allertz et al. and the present study. For instance, Hiraki et al. employed a slag with significantly lower sulfur content

(0.19 mass%), while Allertz et al. utilized a slag with considerably higher Al_2O_3 content (more than 30 mass%). The differences in slag properties and quality may be the factors leading to the differences in desulfurization effects.

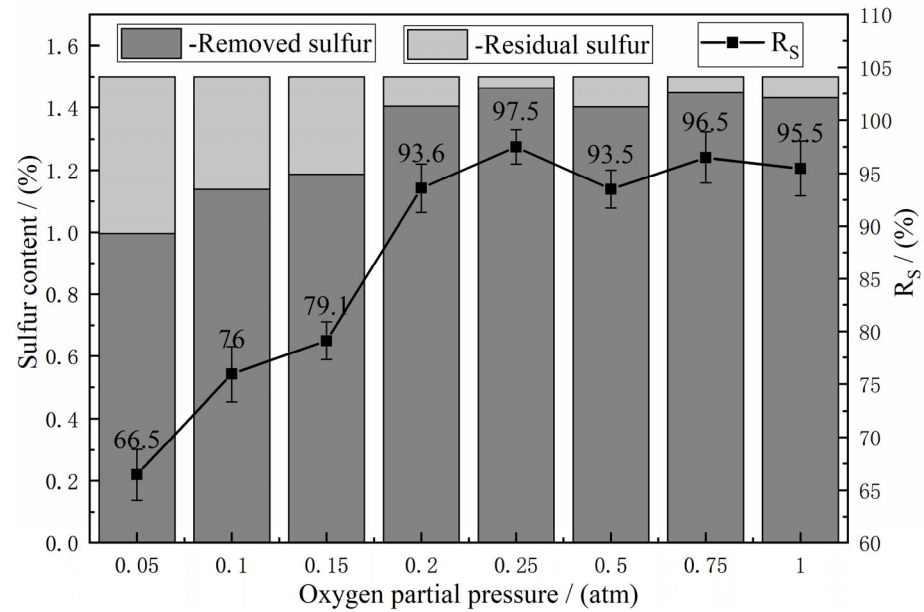


Figure 13. The change in desulfurization rate with oxygen partial pressure after 120 min oxidation of slag.

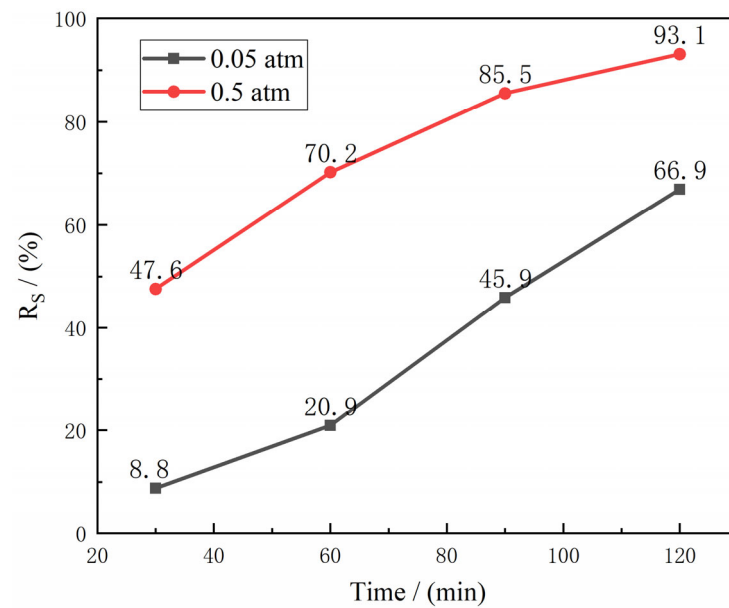


Figure 14. Graph of desulfurization rate of slag with time.

Therefore, at high oxygen pressure ($P_{O_2} \geq 0.20$ bar), the limiting step of the sulfur oxidation process in slag is S^{2-} diffusion control in the liquid phase. At low oxygen pressure ($P_{O_2} < 0.20$ bar), the desulfurization rate increases with the increase in oxygen partial pressure. Therefore, at low oxygen pressure ($P_{O_2} < 0.20$ bar), the limiting step of the sulfur oxidation process in slag is the diffusion control of O_2 in the reaction zone. As the oxygen partial pressure of the system increases, the O_2 content diffused to the slag surface per unit time increases, promoting the full reaction of S^{2-} in the slag and O_2 diffused to the interface coefficient of J_{O_2} to J_S .

Figure 15 illustrates the degree of sulfur removal plotted against reaction time for various conditions. The oxidation condition in Figure 15a is the change in the total flow

of reaction gas in a corundum crucible at 0.5 bar oxygen partial pressure. The oxidation condition in Figure 15b is the change in the type of corundum crucible at a total flow rate of 2 L min^{-1} and 0.5 bar oxygen partial pressure. It can be seen from Figure 15a that gas flow rate has little influence on sulfur removal in slag. This is the same as the pure CaS oxidation rate independent of gas flow rate reported by Kobayashi et al. [21]. The surface area of the slag contained in the Al_2O_3 crucible boats is approximately 200% larger compared to the slag in the Al_2O_3 crucibles. Given this discrepancy, it is reasonable to anticipate an impact on the desulfurization of the slag, as the potential location for Equation (2) directly correlates with the surface area. As can be seen from Figure 15b, these experimental results are in line with the preceding discussion regarding the impact of container form. In summary, the partial pressure of SO_2 in the slag oxidation desulfurization reaction system affects desulfurization, but it is not the main factor.

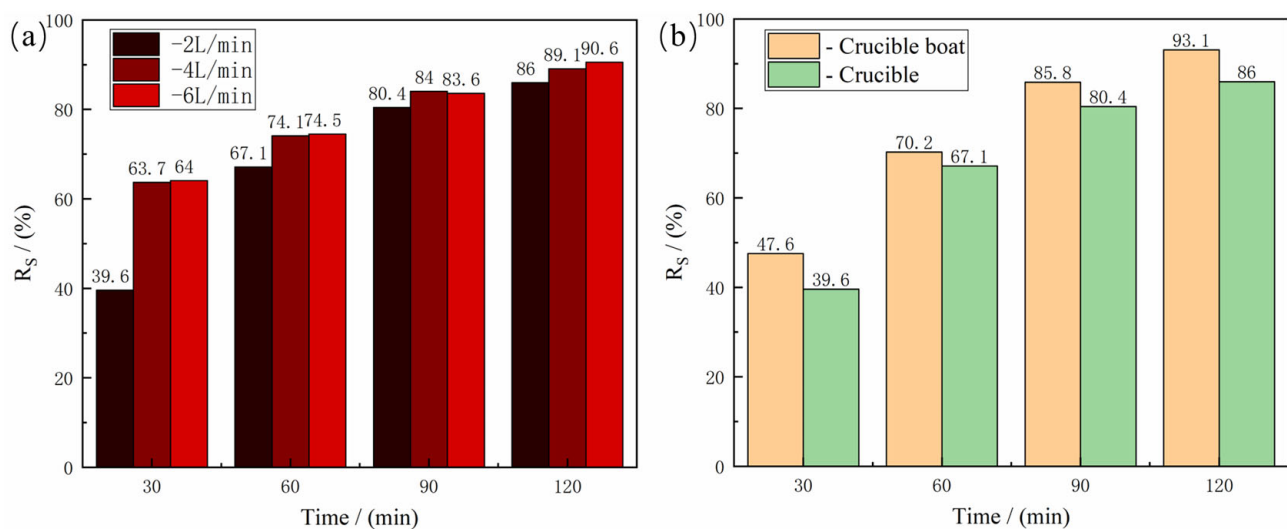


Figure 15. Variation diagram of desulfurization rate of slag with time under different conditions ((a) different gas flow, (b) different crucible shapes).

4.3. Occurrence State of Residual Sulfur after Oxidation of Slag

Based on the analysis of the experimental results above, it is evident that when the oxygen partial pressure of the reaction system was 0.15 bar or less, all oxidized slag samples exhibited the presence of an independently distributed CaS phase within the slag. Furthermore, as the oxygen partial pressure of the system increased, the content of the independently distributed CaS phase in the oxidized slag samples gradually decreased. When the oxygen partial pressure of the reaction system reached or exceeded 0.20 bar, no independently distributed CaS phase was observed in the slag sample. Under high oxygen pressure ($P_{\text{O}_2} = 0.5 \text{ bar}$), it was observed that elemental sulfur became concentrated in the newly formed physical phase 6 ($11\text{CaO}\cdot 7\text{Al}_2\text{O}_3\cdot \text{CaS}$) during the oxidation process. This phenomenon occurred because Ca^{2+} and S^{2-} ions in KR desulfurization slag exhibit low electrostatic potentials at low oxygen pressures ($P_{\text{O}_2} < 0.20 \text{ bar}$), resulting in the formation of CaS ion pairs. This is in line with the findings of He H Y et al.'s [22] investigation on the mechanism of sulfur occurrence in LF refining slag, which discovered that the majority of the sulfur in the slag is present as CaS. Under high oxygen pressure ($P_{\text{O}_2} \geq 0.20 \text{ bar}$), due to the high concentration of oxygen in the oxidation system, the O^{2-} activity in KR desulfurization slag is higher and combines with Ca^{2+} in the slag to form CaO. In the slag, S^{2-} replaces the free exoskeleton O^{2-} in the matrix phase ($12\text{CaO}\cdot 7\text{Al}_2\text{O}_3$) to form the $11\text{CaO}\cdot 7\text{Al}_2\text{O}_3\cdot \text{CaS}$ phase, which exists in the KR desulfurization slag. Similar to this observation, Lv N N et al. [23] reported on the sulfur occurrence in LF refining waste slag and found that $11\text{CaO}\cdot 7\text{Al}_2\text{O}_3\cdot \text{CaS}$ would form when S^{2-} in the slag replaced the free O^{2-} in $12\text{CaO}\cdot 7\text{Al}_2\text{O}_3$.

5. Conclusions

An analysis was conducted to investigate the potential for sulfur elimination through oxidation from the utilized KR desulfurization slag. Experiments were conducted using laboratory-synthesized KR desulfurization slag. Before conducting the studies, the sulfur content and composition of the slag were determined. The initial mass percentage of sulfur in the slag was 1.5%. Experiments were conducted in the gas flow range 2–6 L min⁻¹ and the oxygen partial pressure range 0.05–1.0 bar. After each experiment, the final sulfur content and chemical composition of the slags were analyzed. Based on experimental observations and theoretical analysis, the following conclusions can be drawn.

1. At 1420 °C, under oxidizing conditions, sulfur residue persists in the slag as the CaS phase following oxidation at low oxygen pressure ($P_{O_2} < 0.20$ bar). However, under high oxygen pressure ($P_{O_2} \geq 0.20$ bar), sulfur residue oxidizes from the CaS phase to form the $11CaO \cdot 7Al_2O_3 \cdot CaS$ phase within the slag. The residual sulfur phase in the oxidized slag remains unchanged with varying oxidation times.
2. Under the condition of 1420 °C, the desulfurization rate of slag oxidized for 120 min at low oxygen pressure ($P_{O_2} < 0.20$ bar) increases with the increase in oxygen partial pressure. At high oxygen pressure ($P_{O_2} \geq 0.20$ bar), the desulfurization rate of slag samples does not change with the change in oxygen partial pressure, and the desulfurization rate is higher than 93.5%. However, the rise was rather small. In actuality, sulfur reduction might be accomplished using air.
3. The sulfur removal rate is directly correlated with the slag surface area and the flow rate of the reaction gas, and it increases with an increase in both surface area and gas flow rate.

Author Contributions: Conceptualization, P.J. and R.A.M.; methodology, J.J. and R.A.M.; software, J.J. and R.A.M.; validation, J.J. and P.J.; formal analysis, P.J.; investigation, J.J. and P.J.; resources, J.J.; data curation, J.J. and R.A.M.; writing—original draft preparation, J.J. and J.L.; writing—review and editing, J.J. and J.L.; visualization, J.J. and J.L.; supervision, J.J. and J.L.; project administration, J.J.; funding acquisition, J.L. All authors have read and agreed to the published version of the manuscript.

Funding: This work was financially supported by the National Natural Science Foundation of China (52074199) and the State Key Laboratory of Refractories and Metallurgy, Wuhan University of Science.

Data Availability Statement: The original contributions presented in the study are included in the article, further inquiries can be directed to the corresponding author.

Conflicts of Interest: Author Peng Jiang was employed by the company Jiangsu Yonggang Group Co., Ltd. The remaining authors declare that the research was conducted in the absence of any commercial or financial relationships that could be construed as a potential conflict of interest.

References

1. Nakai, Y.; Sumi, I.; Kikuchi, N.; Kishimoto, Y.; Miki, Y. Aggregation Behavior of Desulfurization Flux in Hot Metal Desulfurization with Mechanical Stirring. *ISIJ Int.* **2013**, *53*, 1411–1419. [\[CrossRef\]](#)
2. Zhu, R.L.; Li, J.L.; Jiang, J.J.; Yu, Y.; Zhu, H. Effect of Basicity on the Sulfur Precipitation and Occurrence State in Kambara Reactor Desulfurization Slag. *Minerals* **2021**, *11*, 977. [\[CrossRef\]](#)
3. Nakai, Y.; Hino, Y.; Sumi, I.; Kikuchi, N.; Uchida, Y.; Miki, Y. Effect of Flux Addition Method on Hot Metal Desulfurization by Mechanical Stirring Process. *ISIJ Int.* **2015**, *55*, 1398–1407. [\[CrossRef\]](#)
4. Nakai, Y.; Sumi, I.; Matsuno, H.; Kikuchi, N.; Kishimoto, Y. Effect of Flux Dispersion Behavior on Desulfurization of Hot Metal. *ISIJ Int.* **2010**, *50*, 403–410. [\[CrossRef\]](#)
5. Moosavi-Khoonsari, E.; Van Ende, M.A.; Jung, I.H. Kinetic simulation of hot metal pretreatment: Desulfurization using powder injection. *Metall. Mater. Trans. B* **2022**, *53*, 981–998. [\[CrossRef\]](#)
6. Li, Q.; Ma, S.; Feng, M.; Lei, H.; Zou, Z. Energy efficiency characterization and optimization of mechanical stirring multiphase dispersion processes: Applied to Kanbara reactors for hot metal desulfurization. *J. Mater. Res. Technol.* **2023**, *24*, 5642–5659. [\[CrossRef\]](#)
7. Ma, N. Trebarent of Hot Metal Desulfurization Slag with CO₂ Gas in the Temperature Range of 873 K to 1473 K for Better Recycling of the Slag. *Metall. Mater. Trans. B* **2024**, *55*, 409–417. [\[CrossRef\]](#)

8. Shiha, Y.F.; Tseng, S.S.; Wang, H.Y.; Wei, C.-T. A Study of the Replacement of Desulphurization Slag for Sand to Ready-Mixed Soil Materials (RMSM). *Comput. Concr. Int. J.* **2016**, *17*, 423–433. [[CrossRef](#)]
9. Tong, Z.B.; Ma, G.J.; Cai, X.; Xue, Z.; Wang, W.; Zhang, X. Characterization and Valorization of Kanbara Reactor Desulfurization Waste Slag of Hot Metal Pretreatment. *Waste Biomass Valorization* **2016**, *7*, 1–8. [[CrossRef](#)]
10. Du, H.; Li, J.; Ni, W.; Xu, D.; Li, N.; Mu, X.; Hou, Y.; Li, Y.; Fu, P. Optimization of the Whole-Waste Binder Containing Molten Iron Desulfurization Slag from Kambara Reactor for Concrete Production. *J. Build. Eng.* **2022**, *54*, 104594. [[CrossRef](#)]
11. Fujino, K.; Ono, K.; Murakami, T.; Kasai, E. Effective utilization of KR slag in iron ore sintering process. *Tetsu-Hagane/J. Iron Steel Inst. Jpn.* **2017**, *103*, 357–364. [[CrossRef](#)]
12. Nakai, Y.; Kikuchi, N.; Iwasa, M.; Nabeshima, S.; Kishimoto, Y. Development of Slag Recycling Process in Hot Metal Desulfurization with Mechanical Stirring. *Steel Res. Int.* **2009**, *80*, 727–732.
13. Kuo, W.T.; Hou, T.C. Engineering Properties of Alkali-Activated Binders by Use of Desulfurization Slag and GGBFS. *Constr. Build. Mater.* **2014**, *66*, 229–234. [[CrossRef](#)]
14. Pelton, A.D.; See, J.B.; Elliott, J.F. Kinetics of Evolution of SO₂ from Hot Metallurgical Slags. *Metall. Trans.* **1974**, *5*, 1163–1171. [[CrossRef](#)]
15. Agrawal, B.; Yurek, G.J.; Elliott, J.F. Kinetics and mechanism of the desulfurization of liquid blast furnace slags by Ar-H₂O gas mixtures. *Metall. Trans. B* **1983**, *14*, 221–230. [[CrossRef](#)]
16. Lynch, D.C.; Elliott, J.F. Analysis of the oxidation reactions of CaS. *Metall. Trans. B* **1980**, *11*, 415–425. [[CrossRef](#)]
17. Jiang, J.-J.; Xiao, C.; Yu, Y.; Li, J.-L. Effect of Temperature on Oxidation Behavior and Occurrence State of Sulfur in KR slag. *JMMB Metall.* **2023**, *59*, 431–441. [[CrossRef](#)]
18. Wei, S.K.; Wang, G.C. Gaseous Desulfurization of Molten Slag in Air Top Blowing Process. *Acta Metall. Sin.* **1965**, *4*, 419–434.
19. Allertz, C.; Du, S.C. Possibility of Sulfur Removal from Ladle Slag by Oxidation in the Temperature Range 1373–1673 K. *J. Sustain. Metall.* **2015**, *1*, 229–239. [[CrossRef](#)]
20. Hiraki, T.; Kobayashi, J.; Urushibata, S.; Matsubae, K.; Nagasaka, T. Removal of Sulfur from CaF₂ Containing Desulfurization Slag Exhausted from Secondary Steelmaking Process by Oxidation. *Metall. Mater. Trans. B* **2012**, *43*, 703–709. [[CrossRef](#)]
21. Kobayashi, K.; Hiraki, T.; Nagasaka, T. Oxidation of Pure Solid CaS with Ar-O₂ Gas Mixture. *High Temp. Mater. Process.* **2012**, *31*, 667–673. [[CrossRef](#)]
22. He, H.Y.; Ni, H.W.; Gan, W.G.; Lin, L. Sulfur Occurrence Form and Formation Mechanism of Sulfur-Containing Phase in Refined Steel Slag. *Steel* **2009**, *44*, 32–35.
23. Lv, N.N.; Yu, J.K.; Suan, C.; Wang, H.Z. Study on Sulfur Occurrence form in LF Refining Waste Residue. *J. Northeast. Univ. (Nat. Sci. Ed.)* **2013**, *34*, 1261–1264.

Disclaimer/Publisher’s Note: The statements, opinions and data contained in all publications are solely those of the individual author(s) and contributor(s) and not of MDPI and/or the editor(s). MDPI and/or the editor(s) disclaim responsibility for any injury to people or property resulting from any ideas, methods, instructions or products referred to in the content.